International Journal of Multiphysics
Volume 18, No. 2s, 2024
ISSN: 1750-9548

Dynamic Obstacle Avoidance Method for 2D Robot with Underwater Actuator in Velocity Vector Coordinate System

Sijun Wu[1†], Zekai Wang[1]

[1] Zhejiang Industry Polytechnic College, Shaoxing, Zhejiang, 312000, China

E-mail: simple990712@126.com (S.W.), wzk2018163@163.com (Z.W.)

Abstract

With the rapid development of China's industry in recent years, marine operations have gradually become the main task of the marine industry, and navigation safety is particularly important in the marine police. This paper proposes a dynamic obstacle avoidance method for underwater robots in a velocity vector coordinate system as an effective solution to such problems, in view of the shortcomings of traditional obstacle avoidance methods such as low efficiency and inability to adapt to the growing underwater robot environment. With the progress of time, people put forward higher and more comprehensive requirements for obstacle avoidance technology, especially in the field of deep-sea exploration, underwater robots as a new highly intelligent automatic production device has received extensive attention from researchers in various countries. The relationship between velocity and displacement in a high-speed kinematic transformation mechanism is non-linear and is transformed by velocity and acceleration information, so the use of the IRP method to study the control laws of mobile robots is of great practical value. In addition, because the fast instantaneous velocity vector coordinate system is accurate, efficient and easy to implement in practice, we use the angle between velocity and direction to establish a three-dimensional adjustable recursive trajectory equation to describe its motion, and then iterate this equation to obtain the obstacle avoidance method.

Keywords: underwater robot; dynamic obstacle avoidance; velocity vector coordinate system; obstacle avoidance strategy; perturbed fluid model; hybrid obstacle avoidance structure

1. Introduction

With the development of society, modern robots have become an indispensable part of people's lives, and they play an increasingly important role in our daily life and work, and the obstacle avoidance method is a very critical part for underwater robots [1]. Because the velocity vector coordinate system has significant advantages over traditional obstacle avoidance methods: accelerometers can accurately measure instantaneous wind speed, torque and moment at rest; precise angular velocity and altitude, so the velocity vector coordinate system is mainly used to study the connection and role of key components such as dynamic planners and accelerometers in the motion control of underwater robots; in order to achieve accurate coordinate transformations, it is possible to To achieve accurate coordinate transformations, the modelling process can be simulated using multi-degree-of-freedom dynamics modelling methods and modern optimisation algorithms [2-3].

An obstacle avoidance system is a special intelligent mobile robot for unmanned control, mainly consisting of sensors, actuators and other auxiliary devices, where the radar signal receiving part is the radar data acquisition,

and the robot visual perception part is the image acquisition and processing module [4]. Obstacle avoidance technology is widely present in industrial manufacturing, in military applications: such as navigation and positioning, guided weapons, etc.; in the direction of civilian life: equipment or tasks that can be used to detect the position of an obstacle and react quickly to make a corresponding decision. The purpose of the obstacle avoidance method is to make the obstacle attracted to the TSP (automatic adaptive balance system) without the use of other protective equipment, human intervention and shielding, interference, etc. [5-7], which can effectively reduce or even eliminate the impact of changes in the vicinity of the target point due to external factors. At present, domestic and foreign research on mobile robot control has made great progress, but for the underwater robot system itself characteristics and environmental conditions dynamic fuzzy, complexity and other issues have not been reported, while there is no a unified standard requirements and implementation scheme design method and program writing method for this topic [8].

Motion control is a key part of the robot and determines the success of the obstacle avoidance system and its ability to operate in complex and variable environments [9]. Since there are no tools such as GURT and HFSS in the velocity vector coordinate system to directly read out the velocity and angular rotation difference, we must first convert the stationary state into a linear running trajectory to identify and determine the distance and direction between the points on the path; then calculate the control vector based on the position information for fast positioning to avoid too large an angle between the target and the obstacle, which affects the obstacle avoidance system to complete the task in a complex and changing environment [10]. The task is accomplished in a complex and changing environment [10]. Based on the analysis of motion control strategies, we can see that the velocity vector-based obstacle avoidance algorithm is a relatively advanced, widely used, stable and reliable method. However, in practice it is not possible to completely eliminate errors. Therefore, it needs to be studied and improved in order to achieve the desired goal of obstacle avoidance and to obtain excellent performance indicators (e.g. high accuracy, good stability, etc.) for the robot in an ideal situation [11].

In global planning due to the vastness of the planning area, the environment can generally be downscaled to a two-dimensional flat map processing, so that although the algorithm avoids the sharp increase in computation when dealing with three-dimensional maps, the whole process inevitably therefore ignores the three-dimensional motion characteristics of the underwater robot in the local space; secondly, the wider sea environment is more complex and some smaller obstacles are often difficult to reflect, as well as some of the environment's Secondly, the large range of sea environments is complex and some smaller obstacles are often difficult to represent, as well as some dynamic obstacles in the environment, which are very detrimental to the navigation safety of underwater robots [12]. To improve the navigability and safety of the planned path, 3D local path planning is often required for underwater robots. The algorithm is mainly used in the field of unmanned aircraft and unmanned boats, and has achieved some results. The author will elaborate on the content of the algorithm, improve on the problems of stationary points and optimisation of reaction coefficients, and apply it to 3D local path planning of underwater robots.

2. Description of environmental information

AUVs navigating in the ocean usually encounter many types of obstacles (e.g. reefs, whirlpools, schools of fish, etc.), the vast majority of which are irregular in shape. To ensure the safety of AUV navigation these irregular obstacles can be simplified by using 3D shapes similar to their form to envelop the obstacles, such as spheres, cylinders, cones, rectangles and other convex bodies. Described by a unified expression as follows.

$$\Gamma_p = \left(\frac{x-x_0}{a}\right)^{2p} + \left(\frac{y-y_0}{b}\right)^{2q} + \left(\frac{z-z_0}{c}\right)^{2t} \qquad (1)$$

where (x_0,y_0,z_0) denotes the coordinates of the centroid of a known obstacle, a, b, c and p, q, r are constants, and combinations of different assignments correspond to convex bodies of different shapes (several common cases are shown in Figures 1-figure supplement 4 below), and it is clear that the region indicated by a result of Eq. 1 less than 1 is the interior of the obstacle, and equation 1 results greater than 1 indicate the surface and exterior of the obstacle.

International Journal of Multiphysics
Volume 18, No. 2s, 2024
ISSN: 1750-9548

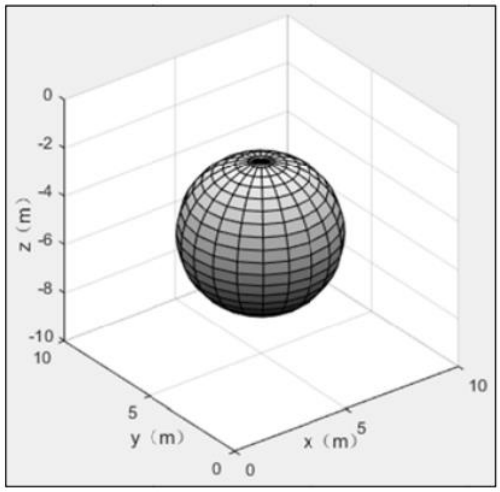

Figure 1 Sphere (satisfying p=q=r=l; a=b=c)

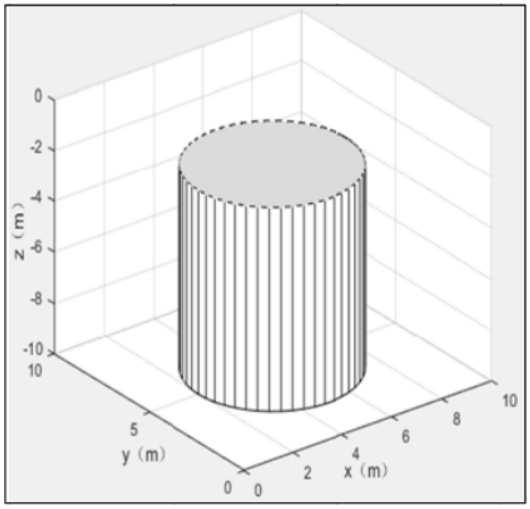

Fig. 2 Cylinder (satisfying p=q=1;r>1;a=b)

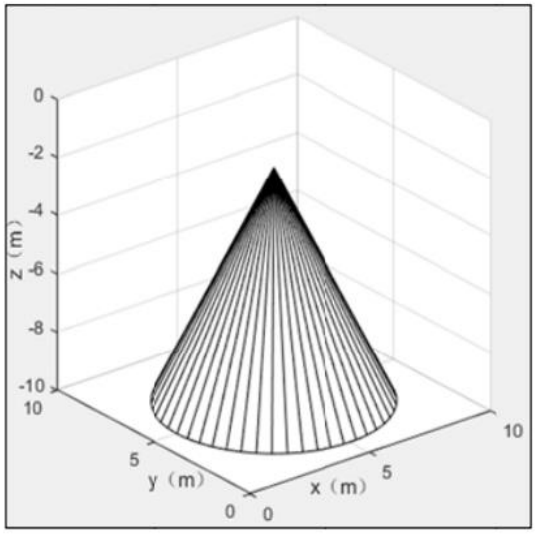

Fig. 3 Cone (satisfying p=y=1;r<1;a=b)

https://doi.org/10.52710/ijm.v18.i2s.933

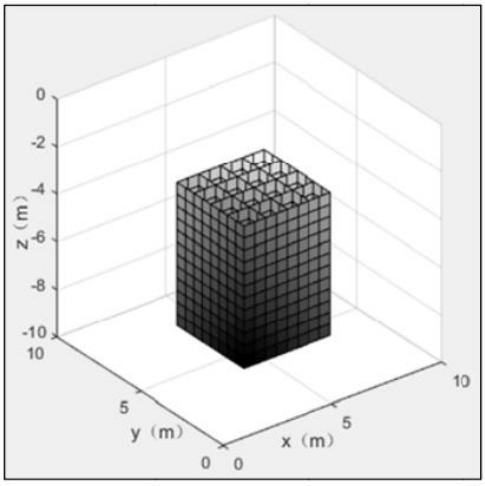

Fig. 4 Rectangular (satisfying p>1;q>1;r>1)

3. Flow field model

3.1 Initial flow field model

The initial flow field model (i.e., undisturbed flow field model) is constructed in the AUV working environment, which can be regarded as a collection of flow bundles converging from all around the environment to the target point g. Since the initial flow field model is set to be undisturbed by obstacles, then according to the guidance of the fluid in the initial flow field, any point p in the environment can reach the target point g along a straight line. The initial flow field model is shown in Figure 5 below.

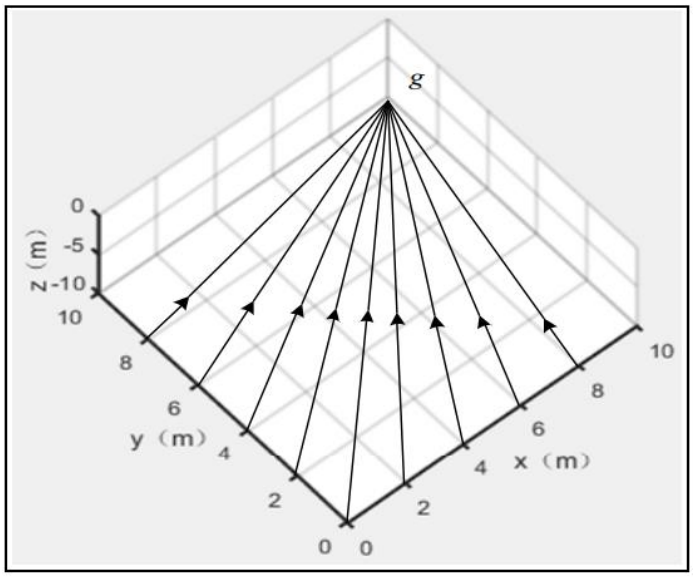

Figure 5: Schematic diagram of the initial flow field model

The expression for the initial fluid vector velocity V(p) passing through each location point in the initial flow field is as follows

$$V(p) = -V\left[\frac{x-x_g}{d(p,g)}, \frac{y-y_g}{d(p,g)}, \frac{z-z_g}{d(p,g)}\right]^T \qquad (2)$$

where V denotes the set fluid convergence rate and d(p, g) denotes the Euclidean distance between any location point p in the environment and the target point g.

$$d(p, g) = \sqrt{(x - x_g)^2 + (y - y_g)^2 + (z - z_g)^2} \qquad (3)$$

Then a virtual point p_4 can be set at the starting position of the AUV, and the line bundle generated through the flow of the virtual point p_4 under the action of the flow field is used as the local planning path of the AUV. $v(p_4)$ then denotes the vector velocity of the virtual point p_4 under the action of the initial flow field. The expression is the same as described in equation (4.2) above, and its value changes as the position of point p_4 in the environment changes. To verify the target accessibility of the resulting path under the action of the initial flow field, a Lyapunov function based on the distance error between the AUV and the target point is established:

$$L = \frac{1}{2} d(p_A, g)^2 \qquad (4)$$

Find the derivative of the distance error function L with respect to time t and substitute equation (2) to obtain:

$$\frac{dL}{dt} = (x - x_g, y - y_g, z - z_g) \cdot \frac{-V}{d(p,g)} [x - x_g, y - y_g, z - z_g]^T \leq 0 \qquad (5)$$

It can be seen that the derivative of the Lyapunov function L with respect to time t is less than or equal to zero, and the system can be stabilised, verifying its target reachability.

3.2 Disturbance flow field model

If there are obstacles in the environment, then these obstacles will inevitably perturb the initial flow field set out above, thus making the initial flow field of fluid convergence direction change, then the flow field model is the perturbed flow field model, from the initial flow field model to the perturbed flow field model of the conversion matrix is called the correction matrix. Let the number of obstacles in the environment be W. Define the total correction matrix M(p) of the perturbed flow field model as follows.

$$M(p) = \sum \omega_w(p) M_w(p)_{w=1}^{W} \qquad (6)$$

where aw(p) and $M_n(p)$ denote the coefficient of perturbation influence of the wth obstacle in this environment on the initial fluid at point p and the corresponding correction matrix. ω(p) and $M_a(p)$ are specifically expressed as follows in equation (7)

$$\omega_w(p) = \{\prod \frac{\Gamma_i(p) - 1}{(\Gamma_i(p) - 1) + (\Gamma_w(p) - 1)}_{i=1, i \neq w}^{W} \qquad (7)$$

It can be seen that the value of the influence coefficient $\omega_a(p)$ is mainly related to the distance from the point p to the obstacle, as well as the external shape and size of the obstacle, and due to the need to normalise ω(p), where the third order unit matrix, also known as the attraction matrix, acts similarly to the gravitational function in the artificial potential field method, and can be considered as the repulsion matrix, acting similarly to the repulsion function in the artificial potential field method.

$$n_w(p) = [\partial \Gamma_p / \partial x, \partial \Gamma_p / \partial y, \partial \Gamma_p / \partial z]^T \qquad (8)$$

The above equation is the radial normal vector perpendicular to and outward from the surface of the wth obstacle; p_n denotes the repulsive response coefficient reflected by that obstacle at point p. Its value is related to the set initial value ρ and the distance 1 from point p to the surface of the obstacle (ρ is a greater than zero constant). pr. The value of pr. has an important influence on the effect of the correction of the matrix M.(p); the larger its value, the sooner the corrected fluid will be able to evade obstacles in the environment sooner. In summary, the initial flow field is modified to obtain the perturbed flow field, and the perturbed flow field model is shown in Figure 6.

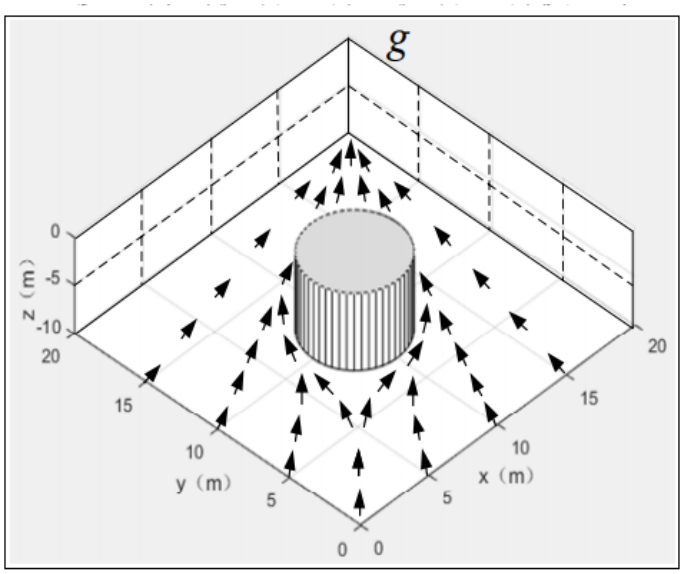

Figure 6: Schematic diagram of the perturbed flow field model

3.3 Relative perturbation flow field model

The traditional perturbed flow field model is only applicable to the static environment, but in the actual working environment the AUV will also be disturbed by various dynamic obstacles, so it is necessary to introduce the concept of relative flow field to guide the AUV in the dynamic environment for path planning. Assuming that there are k dynamic obstacles in the environment that pose a threat to the safety of the AUV and that their motion information can be detected by the AUV through its own mounted sensors, let the actual velocity of the ith, (0<i≤k) of these obstacles be u,, and define its reference motion velocity in the disturbed flow field as v,

$$v_i = e^{\frac{-1}{\lambda}(r_i - 1)} u_i \qquad (9)$$

where (1-r))/ is the exponential decay coefficient, mainly related to the value of λ, (λ>0) and the distance from the AUV to the obstacle, the smaller the reference motion velocity the later the AUV starts dynamic obstacle avoidance. The significance of defining the reference motion speed is: when the obstacle is far from the AUV, the actual motion speed u, after exponential decay to obtain the reference motion speed v, is smaller, can be later to avoid the phenomenon of over-avoidance; when the obstacle is close to the AUV, the reference motion speed approximates the actual motion speed, that is, to ensure the timeliness of obstacle avoidance. Therefore, the reference speed reflects the risk level of collision between the AUV and the dynamic obstacle, the higher the value the higher the possibility of collision and the higher the difficulty of avoidance. Usually each dynamic obstacle in the environment is not related to each other, so it is difficult to accurately grasp the motion information of all dynamic obstacles. In order to solve this problem, this paper considers the dynamic obstacles with the largest reference motion speed from the perspective of collision hazard level, and then avoid the dynamic obstacles of the next level, until all dynamic obstacles in the environment are avoided.

3.4 Improving the standing point problem of the perturbed flow field model

Using the perturbed fluid model for local path planning of the AUV, a smoother path can be obtained in the 3D environment in the vast majority of cases, but due to the characteristics of the algorithm itself derived from the artificial potential field, there will be a standing point problem where the virtual velocity is zero, as shown in Figure 7 below.

International Journal of Multiphysics
Volume 18, No. 2s, 2024
ISSN: 1750-9548

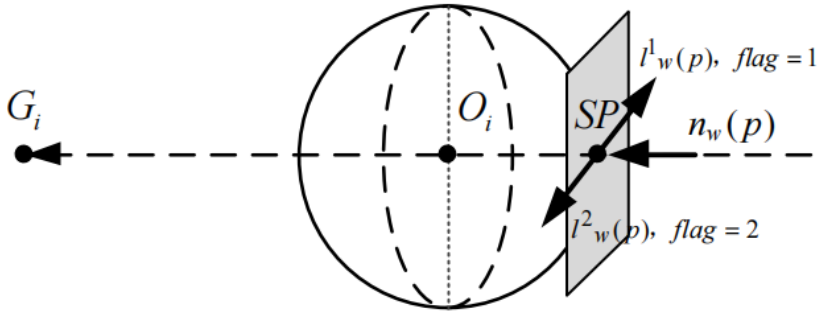

Figure 7: Schematic diagram of the standing point problem

At this point the line between the AUV and the target point is exactly through the centre of the obstacle, the attraction and repulsion velocities are exactly co-linear and reversed, the fluid velocity |V| gradually decreases, when it reaches the surface of the obstacle the velocity decreases to zero that is the stationing point SP, at this point if no intervention is made, the fluid will always stay here. To solve the standing point problem, a possible solution is to attach a correction matrix M^3 in addition to the perturbation matrix M, so that the corrected fluid velocity deviates from the radial vector of the obstacle. As shown in figure (4.4) above, the correction matrix M^3 acts in a plane tangent to the surface of the obstacle perpendicular to the fluid, with the following expressions.

$$M_w^{\perp}(p) = \frac{\tau l_w(p)(n_w(p))^T}{|\Gamma_w(p)|^{\frac{1}{\sigma w}}(n_w(p))^T n_w(p)} \qquad (10)$$

where Z.(p) exists in the tangent plane, is perpendicular to the radial normal vector n.(p), and is mainly chosen to be parallel to the horizontal plane with two component vectors whose values are related to the obstacle avoidance state the vehicle is in, starting positive and ending negative; σ, the tangential response coefficient, is similar to the response coefficient p, above, and is used to determine the timing of the action of the matrix M^3 correction, the larger its value the earlier the timing of the action. The final superimposed correction matrix can therefore be obtained as follows.

$$M_w(p) + M_w^{\perp}(p) = I + \frac{\left((n_w(p))^T n_w(p) I - 2 n_w(p)(n_w(p))^T\right)}{|\Gamma_w(p)|^{\frac{1}{\rho w}}(n_w(p))^T n_w(p)} + \frac{\tau l_w(p)(n_w(p))^T}{|\Gamma_w(p)|^{\overline{\sigma w}}(n_w(p))^T n_w(p)} \qquad (11)$$

The properties of the fluid flow velocity obtained with the new correction matrix still satisfy the above properties. Since the motion of the fluid in a flow field is not limited by almost any kinematic properties, this will result in the algorithm planning a path that does not necessarily satisfy the actual AUV motion constraints. For example, the reaction coefficient ρ, σ determines the timing of the avoidance (i.e. when the fluid deflects) in a perturbed flow field. When the increase is greater than the performance constraints of the underwater robot, the path is not feasible. In order to solve this problem, the response coefficients are adjusted using a rolling optimization strategy. A rolling step of N is used to predict the change in deflection angle within N steps and to determine whether the change in deflection angle at each step exceeds the performance constraints of the underwater robot. Considering that there may be dynamic obstacles in the environment, each step of the prediction requires a local path planning based on the current reaction coefficient to ensure the accuracy of the next prediction.

4. Collision avoidance strategy based on the velocity barrier method

4.1 Collision cone modeling

As shown in Figure 8 below.

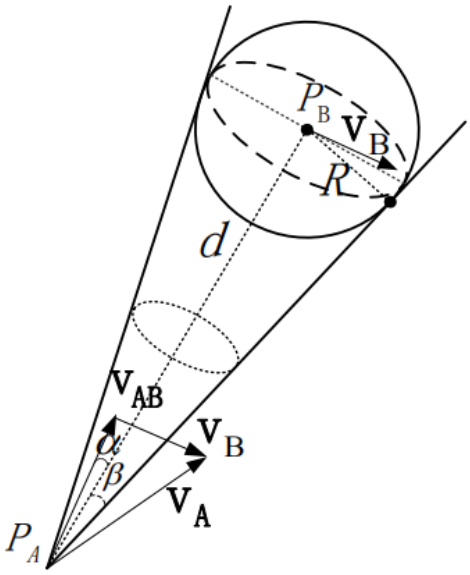

Figure 8 3D collision cone model

It can be seen that the vector velocity of the AUV relative to the obstacle is

$$V_{AB} = V_A - V_B \quad (12)$$

Solve for the angle α between VAB and the axis P₄Pb and solve the following equation to decide whether to take avoidance measures.

$$\alpha = \arccos\left(\frac{V_{AB} \cdot P_A P_B}{V_{AB} \cdot d}\right) \quad (13)$$

$$\beta = \arcsin(R/d) \quad (14)$$

Where β is half the value of the collision cone apex angle, which can be used as an important condition to predict whether a collision will occur, but if the judgement is based on this condition alone there may be over-avoidance, for example when the AUV is far away from the obstacle, although the above angle condition is satisfied, if the avoidance starts too early it will bring additional interference to the path tracking. Therefore to prevent premature obstacle avoidance the following additional constraints are required.

$$t = \min\left\{\frac{\alpha-\beta}{r}, \frac{\alpha-\beta}{q}\right\} \geq \frac{1}{3}\frac{d-R}{V} \quad (15)$$

If the ray in the direction of VAB falls within the collision cone when the constraint is met, then the obstacle is a threat to the navigation of the underwater robot and obstacle avoidance is initiated. If not, no threat exists.

4.2 Determining the obstacle avoidance direction guidance point

Let the underwater robot has met the above collision conditions, in order to simplify the obstacle avoidance model to determine the appropriate direction of obstacle avoidance, the above model along the speed of the obstacle VB direction translation, translation to get three-dimensional velocity obstacle cone model is shown in Figure 9 below.

International Journal of Multiphysics
Volume 18, No. 2s, 2024
ISSN: 1750-9548

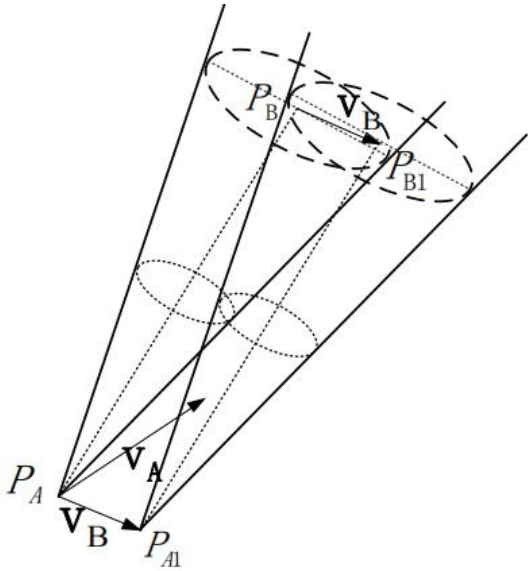

Figure 9 three-dimensional velocity obstacle cone model

The cone of collision is shown in Figure 10 below.

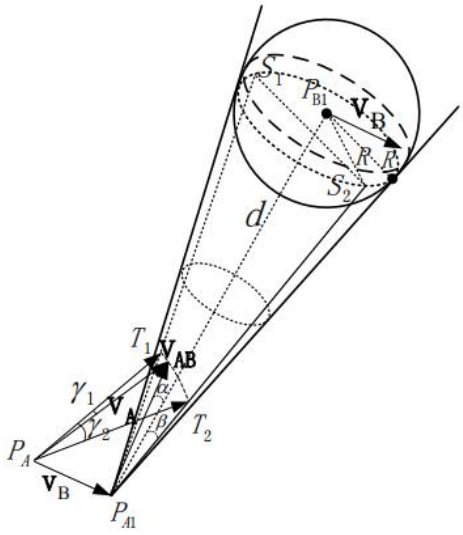

Figure 10 Collision critical point determination

T1 and T2 in the geodetic co-ordinate system can be obtained according to the relationship of the following equation.

$$\cos(\beta-\alpha)=\frac{V_{AB}\cdot P_{A1}T_1}{V_{AB}-P_{A1}T_1} \qquad (16)$$

$$\cos\beta=\frac{P_{A1}P_{B1}\cdot P_{A1}T_1}{d\cdot P_{A1}T_1}=\cos\left(\arcsin(R/d)\right) \qquad (17)$$

$$\cos\langle V_B,\, P_{A1}T_1\rangle=\frac{{V_A}^2-{P_{A1}T_1}^2-{V_B}^2}{2V_B-P_{A1}T_1} \qquad (18)$$

https://doi.org/10.52710/ijm.v18.i2s.933

Subject to the underwater robot motion constraints, the point with the smaller change in velocity direction is selected from the two critical points as the orientation guidance point for the underwater robot, as follows

$$\cos\gamma_1 = \frac{V_A \cdot P_A T_1}{V_A \cdot P_A T_1} \quad (19)$$

$$\cos\gamma_2 = \frac{V_A \cdot P_A T_2}{V_A \cdot P_A T_2} \quad (20)$$

$$if \min(\gamma_1, \gamma_2) = \gamma_1 then T = T_1, else then T = T_2 \quad (21)$$

As the window rolls, whether or not the underwater robot reaches the set T point in this cycle, a new T point will be obtained again in the next cycle based on the current position-velocity relationship, giving the underwater robot a real-time obstacle avoidance direction guidance point until the obstacle avoidance is complete or the collision condition is no longer satisfied.

4.3 Obstacle avoidance guidance and trajectory recovery

As mentioned above, for a sudden obstacle, when the obstacle avoidance direction guidance point is obtained, the underwater robot will navigate with the target point T in this rolling cycle T. At this time, the tracking object of the model predictive control changes from the target point Pr on the reference path to the obstacle avoidance guidance point T . The target function Jobs is optimised to adjust the navigation direction of the underwater robot, which corresponds to the following equation

$$J_{obs} = (X(k) - X_T)^T \cdot D \cdot (X(k) - X_T) \quad (22)$$

Since the position of point T is known at this point, the angular relationship between the underwater robot and point T can be obtained as the reference bow angle and longitudinal inclination of the underwater robot, as shown in Figure 11 below for collision avoidance, where the coordinates OT correspond to the Serret-Frenet coordinate system above, in which the control error is reflected. Also based on the above derivation, the expected value of the velocity direction adjustment of the underwater robot can be obtained as equation (23) below, so that the optimal control input U can be determined from the objective function.

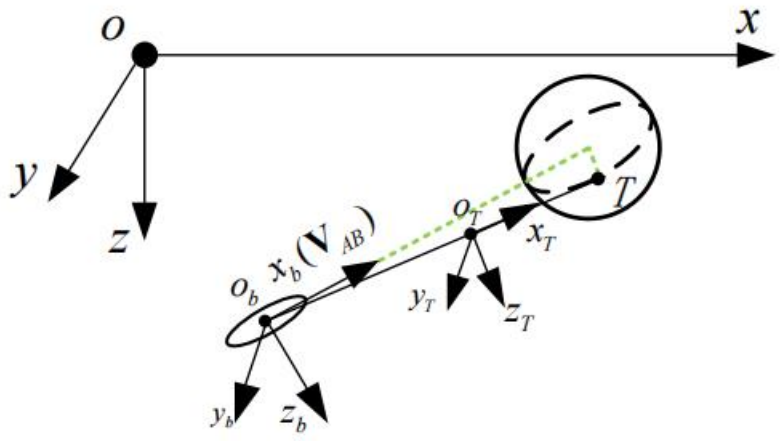

Fig. 11 Schematic diagram of collision avoidance

$$\begin{cases} (\psi(k+1) = \psi_T(k) + acsin\left(\frac{-\varepsilon_y(k)}{\sqrt{\eta_1^2 + \varepsilon_y^2(k)}}\right) \\ \varepsilon_y(k) = -(x - x_\tau)\sin\psi_\tau + (y - y_T)cos\psi_T \end{cases} \quad (23)$$

$$\begin{cases} \theta(k+1) = \theta_t(k) + \arctan\left(\frac{\varepsilon_z(k)}{\sqrt{\eta_2^2+\varepsilon_z^2(k)}}\right) \\ \varepsilon_{(k)} = (x-x_T)\sin\theta_\pi\cos\psi_\pi + (y-y_w)s[\varepsilon_z(k) \\ = (x-x_T)\sin\theta_T\cos\psi_T + (y-y_T)\sin\theta_T\sin\psi_T + (z-z_T)\cos\theta_T \end{cases} \quad (24)$$

$$\mathrm{U} = \begin{cases} r(k+1) = k_\psi \cdot J \cdot \cos\theta\big(\psi(k+1) - \psi(k)\big) + r(k) \\ q(k+1) = k_\theta \cdot J\big(\theta(k+1) - \theta(k)\big) + q(k) \end{cases} \quad (25)$$

5. Conclusion

The key to the velocity vector control algorithm is to determine the optimal motion trajectory. Since underwater robots are confronted with target obstacles in real-world environments and work in harsh environments, they require high positioning accuracy. The distance between the path and the obstacle avoidance point, as well as the difference between their relative stationary velocity values and the time since stationary, need to be accurately calculated to achieve accurate obstacle avoidance. In this paper, we focus on a method of obstacle avoidance based on a velocity vector coordinate system, and introduce the working principle and system components as well as the functions of each part, using an example of an underwater robot in practice. The velocity vector coordinate equations are analysed in detail, and a three-dimensional model is built using MATLAB software, and then the optimal solution at the transient equilibrium point is solved by deriving a linear time-varying non-linear matrix. The velocity vector coordinate system-based obstacle avoidance method designed in this project is based on the values of the velocity parameters set to avoid obstacles when the underwater robot encounters them in actual operation and the maximum velocity to be avoided by the robot in actual operation as the reference standard.

Acknowledgement

Project level: scientific research project of Zhejiang Provincial Department of Education.

Subject name: Hysteresis modeling and compensation control of underwater MFC actuator.Supported by the scientific research project of Zhejiang Provincial Department of Education (Project No.: Y202043865).

References

[1] PANG Shuo, JENG Haifeng. Research progress of intelligent underwater robots[J]. Science and Technology Herald, 2015, 33(23):66-71.
[2] Yao, Shuxiang. A path planning method based on sea current prediction model[D]. Harbin Engineering University, 2019.
[3] Zhu DQ, Yan MZ. A review of path planning techniques for mobile robots[J]. Control and Decision Making, 2010, 25(7):961-967.
[4] Zhang ZW. Research on path planning and obstacle avoidance algorithms for AGVs[D]. University of Electronic Science and Technology, 2018.
[5] Zhang, Nan-Nan. Research on path planning and path tracking methods for underwater robots[D]. University of Science and Technology of Jiangsu, 2019.
[6] Mao YF, Pang YJ. Application of improved particle swarm in underwater robot path planning[J]. Computer Applications, 2010, 30(3): 789-792.
[7] Zhu DQ, Liu Y, Sun B et al. Autonomous heuristic bio-inspired neural network path planning algorithm for autonomous underwater robots[J]. Control Theory and Applications, 2019, 36(2): 183-191.
[8] Wang, Chao, Zhu, Daqi. AUV path planning based on artificial potential field and velocity synthesis[J]. Control Engineering, 2015, 22(3): 418-424.
[9] Ran, X.R.. Research on AUV path planning method based on hierarchical reinforcement learning[D]. Harbin Engineering University, 2017.
[10] Liu Guijie, Liu Peng, Mu Weilei, et al. Path optimization for autonomous underwater robots using energy-optimal improved ant colony algorithm[J]. Journal of Xi'an Jiaotong University, 2016, 50(10): 93-98.

[11] Xu B, Zhang Jiao, Wang Chao. A real-time obstacle avoidance method based on multiple AUV clusters with artificial potential fields[J]. Chinese naval research, 2018, 13(6): 66-71.
[12] DU Pengzhen, TANG Zhenmin, SUN Yan. An object-oriented multi-role ant colony algorithm and its TSP problem solving[J]. Control and Decision Making, 2014(10): 1729-1736.
[13] Yang P, Zhao Z, Zheng HX. Research on global path planning method for mobile robots based on improved ant colony algorithm[J]. Machine Manufacturing and Automation, 2017(06): 161-163+198.
[14] Wang XY, Yang L, Zhang Y, et al. Robot path planning based on improved potential field ant colony algorithm[J]. Control and Decision Making, 2018, 033(010): 1775-1781.
[15] Xia, Z., Yang, X.. Research on ant colony strategy for multi-constrained multi-indicator planning of 3D underwater platform paths[J]. Journal of Military Engineering, 2018, 39(09): 1795-1803.
[16] Ma Ronggui, Cui Hua, Xue Shijiao, et al. Improved ant colony algorithm for optimal path selection with multiple constraints[J]. Journal of Xi'an University of Electronic Science and Technology (Natural Science Edition), 2016, 43(3).